SME Annual Meeting
Feb. 19 - 22, 2012, Seattle, WA

Preprint 12-006

GEOSTATISTICAL ASSESSMENT AND QUANTIFICATION OF UNCERTAINITY OF METHANE IN THE CAVED AND FRACTURED ZONE OF LONGWALL MINES

C. Özgen Karacan, National Institute for Occupational Safety and Health, Pittsburgh, PA

ABSTRACT

The formation of the gas emission zone in longwall mining and the potential amount of gas in this zone are factors of local geology and spatial variability within this geology. Therefore, geostatistical methods can be used for modeling and prediction of gas amounts and for assessing its uncertainty in the gas emission zone of longwall mines.

This study used core data obtained from 64 exploration boreholes drilled from the surface to the bottom of the Pittsburgh coal seam in a mining district in the Northern Appalachian basin. After identifying important coal layers for the gas emission zone, semivariogram modeling was conducted for different coal seams to define the distribution and continuity of various attributes. Sequential simulations were performed for stochastic assessment of these attributes to calculate gas-in-place (GIP) in each coal seam. GIP calculations for coals of various gas emissions zones were combined and ranked for their cumulative distribution function to find GIP in the caved zone and in the fractured zone at the 5%, 50%, and 95% quantiles. Fifty percent quantile results were later used to isolate a panel from the whole area and create a mosaic representation corresponding to the daily advance rate of the longwall face. This approach helped to estimate the daily emissions of this panel from the caved zone and from the fractured zone.

Results showed that gas-in-place in the Pittsburgh coal seam, in the caved zone, and in the fractured zone showed spatial correlations that could be modeled and estimated using geostatistical methods. This study showed that gas-in- place volumes in the study area may be as high as 12.3 Bscf and as much as 3.5 MMscf per acre of mining.

INTRODUCTION

Methane emissions above a longwall coal mine are closely related to the geology of the coals, their properties, and their distances from mining activity. When there is sufficient gas within the gas emission zone, the danger of a methane explosion due to methane inflows may increase if the ventilation and degasification system are not properly designed.

The common gas sources in the overlying formations are caved or fractured coal seams. Strata below the mined seam may also be a major gas source if they contain gassy seams or gassy sandstones. At this juncture, it is important to make an assessment of the gas-in-place within the gas emissions zone. This information can be used to predict the likelihood of sudden gas releases and changes in emissions rates, as well as design surface methane control systems.

Gas emissions zone sizes and emission potentials at various heights above the coal seam have been previously described (Noack 1998; Thakur 2006). These studies show the degree of gas emissions as a function of varying distance from the mined coal bed in overlying and underlying formations. In addition to these studies, Karacan and Goodman (2011) conducted a probabilistic study for a mining district in Southwestern Pennsylvania in the Northern Appalachian basin based on the displacements measured in gob gas ventholes (GGVs) to define the size of the gas emissions zone of the Pittsburgh coal seam during mining operations. Although this study did not consider spatial distribution due to lack of sufficient data, it showed that the deformed zone may extend as high as 350-400 ft above the Pittsburgh coal seam, and the probability of obtaining specific strata displacements may vary based on the proximity of the formation to the Pittsburgh coal seam.

In all studies dealing with a gas emission zone and its size, three major zones were considered: a caved zone, a highly fractured zone, and a composite beam zone. These zones are important for gas emissions and transport into the mining environment, provided that there are sources with high methane amounts within these intervals. Core analyses and geophysical logging techniques are two of the important data sources for characterizing the geological formations and their gas contents in the gas emission zone (Karacan and Diamond 2006). Determinations of reservoir and geomechanical properties of the formations are important because they affect fluid flow and storage in the overburden before and after coal extraction as the stress and strain states change as a result of longwall operations. Thus, laboratory analyses of available core materials from boreholes and accurate borehole logs of coal measure rocks are necessary for any emissions prediction (Karacan 2009). However, laboratory analyses on cores of sampled locations, although beneficial, provide data only from point locations.

This study deals with providing continuity over the area of interest using pointwise data. For this objective, geostatistics and geostatistical modeling are unique methods to establish spatial correlations in sampled data to form continuity, to enable precision, and to assess the uncertainty of the attributes that are being investigated (Webster and Oliver 2007). Geostatistics can be used to account for a wide range of data of varying resolution, quality, and uncertainty for reconciling data types at different scales and for constructing models of geological heterogeneity (Leuangthong et al. 2008). These data and models can later be used as inputs for solving dynamic problems such as flow models.

STUDIED MINING DISTRICT AND ITS GAS EMISSION ZONE

Coal seams as methane sources within the gas emissions zone of longwall mines in the studied district

The studied longwall mining district is located in the southwestern Pennsylvania section of the Northern Appalachian Basin (Figure 1). Markowski (1998) reported that the main coal beds, which are consistent and continuous in the study area of this paper, are the Pittsburgh (PCMB), Sewickley (SWC), and Waynesburg (WBC) coal beds. In addition, the Uniontown coal bed (UNC) and Pittsburgh rider coal beds (PCR) were also present, although not consistently. The Redstone coal (RDC) seam was not observed in any of the core holes and was not included in the calculations. The general stratigraphic log of the area shown in Figure1 is given in Figure 2.

The mining district that was modeled in this work hosted panels with 1,450-ft in width and 12,000-13,000 ft in length. The panels are shown in Figure 1. The dimensions of the area shown in this figure are 8,625 ft in the y-direction (Northing) and 17,325 ft in the x-direction (Easting). In this district, overburden depths ranged between 700 and 1,000 ft.

In regard to coal mine methane and methane emissions into the mines operating the Pittsburgh coal seam, the Monongahela Group of formations (Figure 2) lies within the gas emission zone as defined by Karacan and Goodman (2011) and the PCMB, PCR, SWC, UNC, and

WBC coal beds play key roles in providing the gas-in-place for emissions into mines. However, these seams exist in different parts of the gas emissions zone and thus should be controlled by different components of the ventilation system. For instance, the Pittsburgh coal bed (PCMB) is the main coal bed that is mined. Due to their proximity to the main Pittsburgh coal bed, the Pittsburgh rider coals are usually within the caved volume, and their gas emissions are handled by the ventilation system. Conversely, the Sewickley (SWC), Uniontown (UNC) and Waynesburg (WBC) coals are sufficiently far from the main Pittsburgh seam that they are part of the fractured section of the gas emissions zone as depicted in Figure 2. Therefore, their potential gas emissions should be captured using gob gas ventholes.

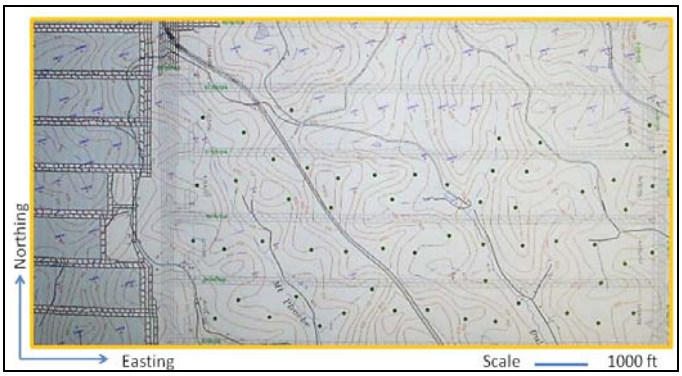

Figure 1. Panel district studied in this paper and layout of the panels.

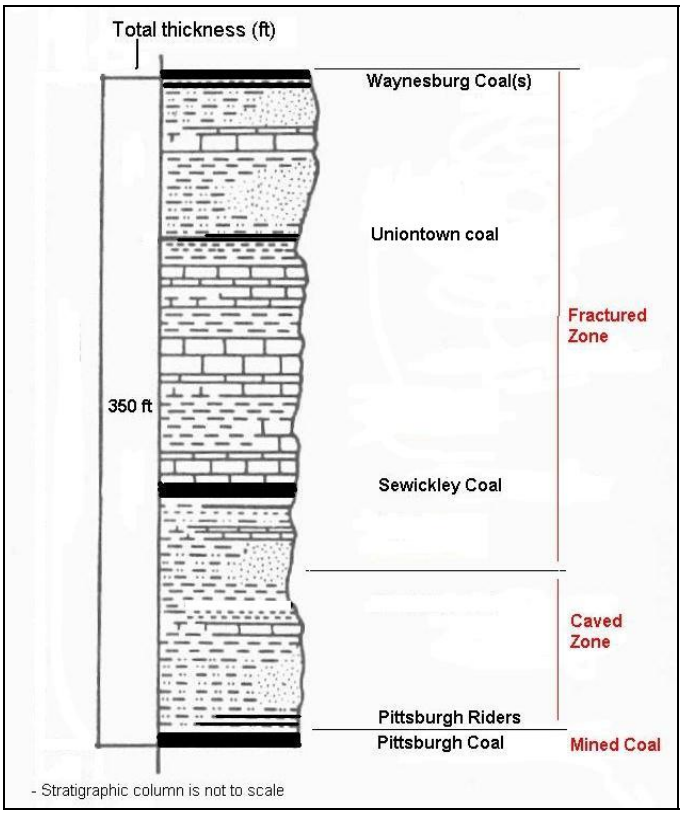

Figure 2. General stratigraphic column that shows the coal seams within different sections of the gas emission zone of the longwall mines given in Figure 1.

Calculation of gas-in-place of coals

One of the key steps in forecasting gas emissions during and after mining is to calculate the volume of gas-in-place (GIP) that will potentially migrate to the underground mining environment. GIP is usually determined by a volumetric method given in Equation 1 (Karacan and Diamond, 2006). Volume-based calculations may also be used to determine the gas-in-place for coal beds in a specific geographic area. This approach both relates the volume of gas in the reservoir at in situ conditions to the volume at surface conditions and treats separately the volume of free gas in fracture porosity (first part of Equation 1) and adsorbed gas in bulk volume.

$$GIP = Ah\left(\frac{43560\phi_f\left(1 - Swf_i\right)}{Bg_i} + 1.359\ GC\ \rho\left(1 - f_a - f_m\right)\right) \quad (1)$$

where:

GIP is the gas in place (Mscf); *A* is the area (acre); *h* is the thickness of coal; φ_f is the fracture porosity (fraction), B_{gi} is the gas formation volume factor (rcf/Mscf); S_{wfi} is the interconnected fracture water saturation (fraction); *GC* is the gas content of the coal (scf/ton); ρ is the coal density (g/cc); f_m is moisture content (fraction); f_a is ash content (fraction); both 43,560 (ft^2/acre) and 1.359 [(Mscf)(ton)(cm^3)/(ac-ft)(scf)(g)] are conversion factors.

Usually the amount of gas stored in fractures is relatively very small. Therefore, in this work, a pseudo-volumetric method was used to calculate gas-in-place for coal seams that encountered only the GIP due to sorbed gas in bulk volume. In this formulation, the undetermined value for f_m was cancelled as well.

$$GIP = Ah\ GC\ \rho\left(1 - f_a\right) \quad (2)$$

In this equation, *GC* is the gas content of coal, *A* is the area (ft^2), "*h*" is thickness of a particular coal bed of interest at a specific point (ft), f_a is the ash content of coal, and ρ is its bulk density (g/cc). In order to obtain GIP in terms of MMscf with these units, this equation should be divided by 35,314,237.3.

The gas content of coal can be measured or estimated using various techniques which usually fall into two categories: (1) direct methods which actually measure the volume of gas released from a coal sample (preferably wire line core) sealed in desorption canisters, and (2) indirect methods based on empirical correlations or laboratory-derived gas storage capacity data from sorption isotherms. Karacan and Goodman (2011) determined the gas content of the main Pittsburgh coal seam and overlying seams by analyzing bivariate normal distributions. The bivariate normal probability calculations and representations of probabilities for obtaining gas contents less than or equal to 350 scf/ton with four-parameter logistic functions were used to estimate gas contents. Means (μ) and standard deviations (σ) of gas content and overburden depth and the correlation coefficients (ρ) between variable pairs that were used in calculating joint probability distributions for gas content and depth are given in Table 1. These analyses showed that gas content of coals could be represented by the values of a dependent variable at 50% value of the independent variables (50% quantile, Q50) of these sigmoid functions up to an overburden of 1,400 ft. The polynomial representation of these coefficients gives a Pearson's correlation coefficient of 0.9969 and is also given in Table 1.

Table 1. Mean (μ) and standard deviation (σ) of gas content (GC) of coals and overburden depth and the correlation coefficients (ρ) between variable pairs used in calculating joint probability distributions.

Data pairs (means and standard deviations)		Correlation	Gas content (scf/ton) equation
Gas content (scf/ton)	Overburden (ft)		
μ = 122.700 σ = 54.766	μ = 588.837 σ = 233.564	c = 0.558	$-5.0E\text{-}5x^2+0.125x+44.328$

Ash content is strongly dependent on the primary paleodepositional environment, the changes in the climate and various precipitations during peat-forming process, and present hydrogeology of the area at a particular depth. Ash is a constituent of coal that does

not have a significant methane sorption capacity. Therefore, its amount should be determined for GIP calculations (Equations 1 and 2). In addition, ash has a higher density than organic matter (112.4–137.4 lb/ft^3; 1.8–2.2 g/cc), and thus ash content is one of the factors that most influences density of coal.

Ash content of important coals in the study area was also determined using bivariate normal distributions, which required bivariate distribution analyses of two random functions for determining joint probabilities of the occurrences of different values. Table 2 gives the resulting equations for ash contents of PCMB, PCR, SWC, UNC and WBC for Q50.

Table 2. Mean (μ) and standard deviation (σ) of ash content of different coals and their overburden depth and the correlation coefficients (c) between variable pairs used in calculating joint probability distributions.

Coal	Data pairs (means and standard deviations)		Correlation	Ash content (%) equations
	Ash content (%)	Overburden (ft)		
PCMB	μ = 7.78 σ = 3.03	μ = 702.98 σ = 195.72	c = -0.0045	9E-07x^2 - 0.0021x + 9.046
PCR	μ = 19.55 σ = 6.86	μ = 609.58 σ = 142.42	c = -0.1220	4E-06x^2 - 0.0076x + 24.06
SWC	μ = 12.00 σ = 3.18	μ = 674.72 σ = 168.78	c = -0.2610	3E-06x^2 - 0.007x + 16.258
UNC	μ = 22.72 σ = 5.39	μ = 468.46 σ = 160.94	c = -0.0647	3E-06x^2-0.0095x+25.010
WBC	μ = 19.62 σ = 4.74	μ = 526.38 σ = 204.21	c = -0.1760	8E-07x^2-0.0052x+22.038

DATA PREPARATION AND MODELING METHODOLOGY

Data preparation

The data that was used in geostatistical modeling was obtained from 64 vertical exploration boreholes drilled over the mining area shown in Figure 1. These boreholes and their spatial locations are shown in Figure 3. For modeling that will be discussed in detail in the forthcoming sections, these data were assigned to a 100 x 50 Cartesian grid in which each grid was 175 ft in the x-direction and 176 ft in the y-direction.

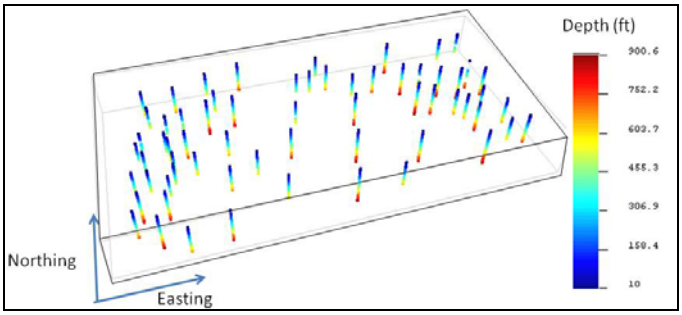

Figure 3. Spatial locations of the boreholes drilled over the area shown in Figure 1 and depths of all identified formations from surface. In this figure, the x-direction is Easting, and the y-direction is Northing.

Because the top of the gas emission zone for mines operating in the Pittsburgh seam extended to a height of 350 ft (Mazza and Mlinar 1977; Karacan and Goodman 2011), the data beyond this interval was excluded from further analyses. Thus, Figure 3 shows only the coal and noncoal layers within the expected gas emissions zone. In this figure, each data point represents an identified formation, and different colors represent their depth from the surface.

To calculate gas-in-place in coals and in different sections of the gas emission zone, the coal beds within the 350-ft interval from the Pittsburgh coal seam, including the Pittsburgh coal seam itself, were identified and isolated from the rest of the data as separate data sets. These coal beds included the Pittsburgh seam (PCMB, main bench), Pittsburgh rider seams (PCR), Sewickley coal (SWC), Uniontown coal (UNC), and Waynesburg coals (WBC, both upper and lower seams). For coal seams of interest, two attributes were determined at each spatial position for geostatistical modeling and for calculation of gas in place using Equation 2. These attributes were overburden depth and thickness of coal. Results of univariate statistical analyses of these data for each coal seam are given in Table 3.

Ash content values calculated for individual seams were later converted to their bulk densities using the correlation that was established for these same coals using the data given in Table 2. Conversion of ash content to bulk density was performed by use of Equation 3.

$$\text{Density (g/cc)} = 0.0001(\text{Ash})^2+0.0028(\text{Ash})+1.3019 \quad (3)$$

The data given and extracted using the procedure given in this section were used to compute GIP in each coal, and later in each section of the gas emission zone, using Equation 2.

Table 3. Univariate statistical parameters of depth and thickness for PCMB, PCR, SWC, UNC and WBC.

DEPTH (ft)	Pittsburgh (PCMB)	Pitts. Riders (PCR)	Sewickley (SWC)	Uniontown (UNC)	Waynesburg (WBC)
Data	**64**	**56**	**62**	**30**	**63**
Mean	686.07	669.08	580.73	405.97	346.14
St. Dev.	129.85	127.44	130.62	139.44	127.47
Variance	16861.60	16240.20	17061.35	19443.67	16247.78
Minimum	435.85	426.72	341.73	192.70	103.60
Maximum	900.58	889.68	803.79	641.00	569.15
THICKNESS (ft)					
Data	**64**	**56**	**62**	**30**	**63**
Mean	6.90	2.41	3.50	0.27	5.37
St. Dev.	0.445	1.160	1.994	0.088	0.585
Variance	0.198	1.347	3.979	0.008	0.343
Minimum	6.14	0.06	0.33	0.10	3.60
Maximum	7.95	5.05	6.90	0.50	6.99

The frequency distributions of the data (histograms) of each of these attributes for coal seams were also checked for their Gaussian behavior. Olea (2009) and Remy et al. (2009) state that for some of the geostatistical modeling and simulation techniques to be applicable without the need of transformation of the data, the data should follow a Gaussian (normal) distribution. Because the distributions of depth and thickness (primary spatial attributes) data were not Gaussian, the data were transformed to normal scores by targeting a Gaussian distribution with mean 0 and variance 1. Semivariograms were then modeled on the normal-score data. However, the values of the attributes were transformed back to the original space during simulations by targeting the original distribution.

Geostatistical modeling of target attributes of coals

For geostatistical simulations, Stanford University Geostatistical Modeling Software (SGeMS) was used for spatial correlation analyses and for stochastic simulations. SGeMS was developed by Stanford Center for Reservoir Forecasting and implements several geostatistical algorithms for modeling of earth systems and phenomena that exhibit space-time distributions (Remy et al. 2009). In addition, this software includes in its platform several of the algorithms that are in the Geostatistical Software Library (GSLIB) (Deutsch and Journel 1998).

Semivariogram analyses. Semivariogram analysis is a method used to examine if the data is correlated with distance. If there is a spatial correlation in the data set, directional semivariograms should start from low values and increase up to the variance of the sample data. The knowledge of spatial correlations and the ranges over which such correlations are observed, along with the knowledge of the mean of the data, is considered by estimating the spatial distribution of parameters and their uncertainty within the Cartesian grid domain by implementing stochastic methods such as sequential Gaussian simulations.

The semivariogram, $\psi(\mathbf{h})$, measures the average dissimilarity between two variables, for example between the values of a parameter ($\mathbf{x}$) at location $\mathbf{u}$ and at a location $\mathbf{u} + \mathbf{h}$. Assuming stationarity, the semivariogram ψ ($Z(\mathbf{u})$, $Z(\mathbf{u} + \mathbf{h})$) depends on a lag vector $\mathbf{h}$: ψ ($\mathbf{h}$). Thus, the experimental semivariogram is computed by (Remy et al. 2009):

$$\psi(\mathbf{h}) = \frac{1}{2N(\mathbf{h})}\sum_{\alpha=1}^{N(\mathbf{h})}[z(\mathbf{u}_\alpha) - z(\mathbf{u}_\alpha + \mathbf{h})]^2 \quad (4)$$

In this description, z ($\mathbf{u}$) is the value of the parameter at location $\mathbf{u}$, and N ($\mathbf{h}$) is the number of data pairs separated by vector $\mathbf{h}$. Semivariograms established using this approach on field or spatially distributed experimental data are generally called empirical or, more conventionally, experimental semivariograms.

Experimental semivariograms, whose data are usually scattered, are modeled with analytical functions (called analytical semivariograms). The most common analytical semivariograms that can either be used by themselves or as nested structures to describe more complicated experimental semivariograms are:

1. Spherical model with range "*a*":

$$\psi(\mathbf{h}) = \begin{cases} \frac{3}{2}\frac{\|\mathbf{h}\|}{a} - \frac{1}{2}\left(\frac{\|\mathbf{h}\|}{a}\right)^3 & \text{if } \|\mathbf{h}\| \le a \\ \psi(\mathbf{h}) = 1 & \text{otherwise} \end{cases} \quad (5)$$

2. Exponential model with practical range "*a*":

$$\psi(\mathbf{h}) = 1 - \exp\left(\frac{-3\|\mathbf{h}\|}{a}\right) \quad (6)$$

3. Gaussian model with practical range "*a*":

$$\psi(\mathbf{h}) = 1 - \exp\left(\frac{-3\|\mathbf{h}\|^2}{a^2}\right) \quad (7)$$

The upper bound of an analytical model is called the "sill." The range is the lowest lag at which the semivariogram reaches the sill; the distance at which 95% of the sill is reached is called the "practical range," as in the case of exponential and Gaussian models.

In this study, semivariogram modeling was performed on the normal-score distribution of each of the attributes (Olea 2006). Details of normal-score transmation are given in Deutsch and Journal (1998). Directional experimental semivariograms of normal scores were searched at 0°, 45°, 90°, and 135° starting from North and changing towards the East direction of lag vectors. In addition, an omnidirectional semivariogram was modeled. In the analytical model search process, attention was given to find a model that would best describe each of these semivariograms. Lag separation distances, the number of lags and lag tolerance, were different in each case, though depending on the nature of the data and the spatial correlations shown by the data.

The experimental semivariogram for the normal-score data of SWC depth and the analytical semivariogram modeling the data is shown in Figure 4, as an example of the attributes modeled in this study.

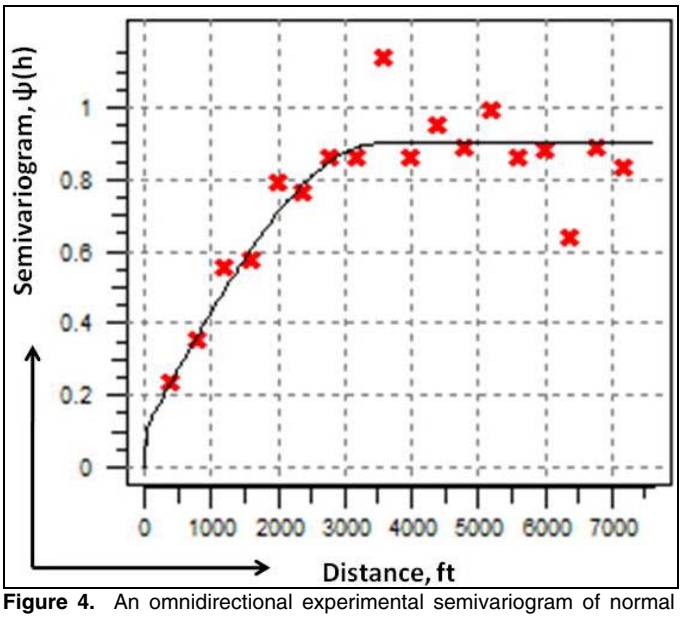

Figure 4. An omnidirectional experimental semivariogram of normal scores of SWC depth and the analytical exponential semivariogram representing the data.

The analytical semivariogram models of the variables for the five coal seams are summarized in Table 4. Please note that the types of the models, their nugget parameters which describe the starting point of the semivariogram, and sills, as well as geometric ranges, all depend on the geological unit and the related attributes.

Table 4. Summary of parameters that describe analytical semivariograms for depth and thickness attributes for PCMB, PCR, SWC, UNC, and WBC. All semivariograms were analyzed using normal-score data and were described with one nested structure.

DEPTH (ft)	Pittsburgh (PCMB)	Pitts. Riders (PCR)	Sewickley (SWC)	Uniontown (UNC)	Waynesburg (WBC)
Model	Spherical	Spherical	Spherical	Exponential	Exponential
Nugget	0.05	0.10	0.10	0.10	0.10
Sill	0.90	0.82	0.80	0.70	0.80
Maximum range	3936	3608	3528	5400	4080
Medium range	3648	3520	3384	5100	4020
Minimum range	3168	3432	3168	4950	3780
THICKNESS (ft)					
Model	Gaussian	Exponential	Spherical	Gaussian	Spherical
Nugget	0.30	0.10	0.10	0.07	0.30
Sill	0.70	0.60	0.50	1.00	0.60
Maximum range	6800	4680	5580	3850	3300
Medium range	6640	4440	5580	3700	3150
Minimum range	6480	4320	5580	3500	3075

Sequential Gaussian simulations and analyses of data. Sequential Gaussian simulation (SGSIM) is a semivariogram-based simulation technique and a special case that takes advantage of convenient properties of Gaussian random functions. Simulated results, or realizations, draw the spatial patterns to be generated from the input data and semivariograms. Realizations can be seen as numerical models of possible distributions of the simulated property in space.

In this work, 100 realizations for each attribute of interest were generated by changing the seed number before the SGSIM of each attribute. In practice, these realizations take the form of a finite number of simulated maps with equal probability to represent the unknown true map. Therefore, each grid in each of these realizations, or simulated maps, generates a distribution of the particular attribute. These distributions can be used to analyze the data statistically for variances and to evaluate the uncertainty associated with various values in a probabilistic fashion. Thus, if proper modeling of confidence intervals and quantiles is an important objective of a study, it is more adequate to use stochastic simulation. In this study, 100 realizations, each of which had 5,000 grid cells, were used for analyses of uncertainty and distribution of properties.

RESULTS AND DISCUSSION

All modeling studies and their results require some level of verification. In this study, the results of sequential Gaussian simulations of modeled attributes (thickness, overburden depth) were compared to the original data before proceeding with calculations of gas-in-place and the associated uncertainties. These comparisons required Q-Q plots of hard data along with SGSIM realizations. Q-Q plots are used to compare probability distributions. A straight line is an indication of equality between the distributions being compared and verification that the data in both axes have similar quantile values (Krishnamoorthy, 2006).

Figure 5 shows, as an example, a Q-Q plot prepared from the hard data of the SWC depth versus its simulated values from one of the realizations of SGSIM. This figure shows that the analyses conducted in this work gave acceptable linear trends between hard data and realizations. This indicates that the probability distributions of these two data sets are almost the same, and that SGSIM produces representative simulated distributions of probability distributions of actual data.

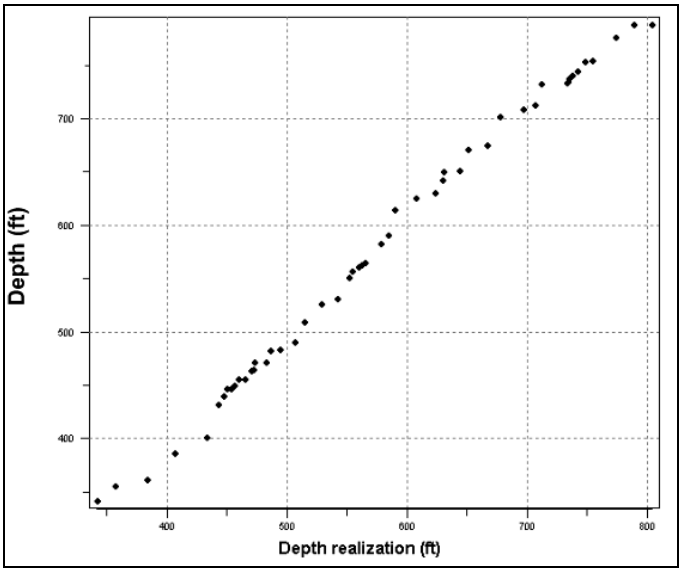

Figure 5. Q-Q plot of depth of Sewickley coal (SWC) against the data of the 50th realization from SGSIM.

Gas-in-place results in the emission zone and their uncertainties

Because the spatial features and their uncertainty impact the predictions of gas-in-place and methane inflows from the gas emission zone, SGSIM results were further analyzed for gas-in-place in the gas emission zone.

In this work, the values of gas-in-place for individual coals and longwall gob zones were calculated at 5%, 50%, and 95% quantiles (Q5, Q50, Q95). These quantiles represent the ranking of the estimated attribute, where each estimated value has the 5th, 50th, and 95th place in ranking analyses. In other words, the estimated values of 5%, 50%, and 95% have a probability to be lower than the actual unknown value. Therefore, the data at 5% quantile are the estimated values at 5% probability, and can be considered as the lower limit. Similarly, the Q95 data has a 95% chance of being higher than the actual value and is considered as the upper limit. Between these, Q50 has a special meaning representing the median of the possible population distribution. Q50 is called the M-type where each estimated value has a 50% chance to be higher than the actual value.

For calculation of gas-in-place (GIP), Equation 2 and the ancillary correlations with the SGSIM realizations of depth and thickness (given in the previous sections) were used. The terms of Equation 2 in each grid were obtained from simulations (thickness and depth) over the simulation area "A." Density, gas content, and ash content values were calculated using their correlations to SGSIM-calculated overburden depth in each grid. These calculations were conducted for all coals within the gas emissions zone of the study area. In order to focus on individual zones, the GIP in PCMB, PCR, and fractured zone (as a combination of SWC, UNC, and WBC) were evaluated and will be presented in the rest of this paper.

To quantify the GIP in each of these coals/zones, 100 GIP realizations were generated for each PCMB, PCR, and fractured zone. By using the cell values within these realizations, total GIPs were calculated for each realization of the total model area, which was 3,535 acres. The GIP values of the realizations were ranked, and percentile analyses were conducted on their histogram to extract the realizations that correspond to Q5, Q50, and Q95. Figure 6 shows the rankings of all 100 realizations for PCMB and selections of Q5, Q50, and Q95 values of total GIP.

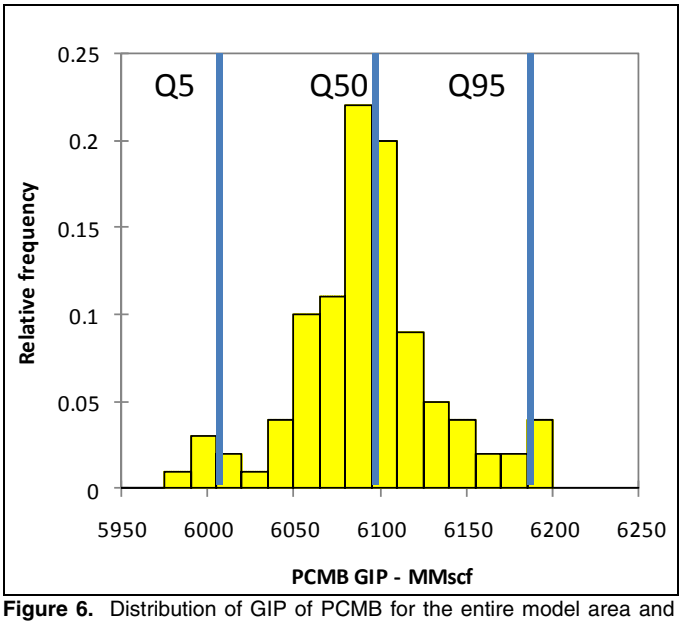

Figure 6. Distribution of GIP of PCMB for the entire model area and locations of Q5, Q50, and Q95. These data are based on all data points of 100 realizations.

GIP, uncertainties, and application to longwall mining

Gas-in-place in coal seams, its spatial distribution, and uncertainty associated with estimations have direct relations and consequences to longwall mining. Figure 7 shows the realizations that give Q50 for the PCMB, PCR, and fractured zone in this study. As apparent from these realizations of gas-in-place, there are regions that will likely result in more gas during mining, both from the lower seams and from the fractured zone. For instance, the right side of the model area at the PCMB horizon is gassier and may require more ventilation during mining, as opposed to the left side of the model area. The GIP per acre of mining for PCMB in this area is 1.334 MMscf (minimum), 2.076 MMscf (maximum), and 1.705 MMscf (mean). Similarly, the left and right sides of the PCR rider seam are gassier compared to the middle and may result in higher emissions to the mine when it caves. This may also result in more methane buildup after sealing. The minimum, maximum, and mean GIPs per acre of mining for the PCR

are 0.007, 0.623, and 0.244 MMscf, respectively. At this point, readers should be advised that the color scale in this map is based on the GIP values in each cell of the maps, not per acre of mining. Therefore, per-acre values are not shown in color scales.

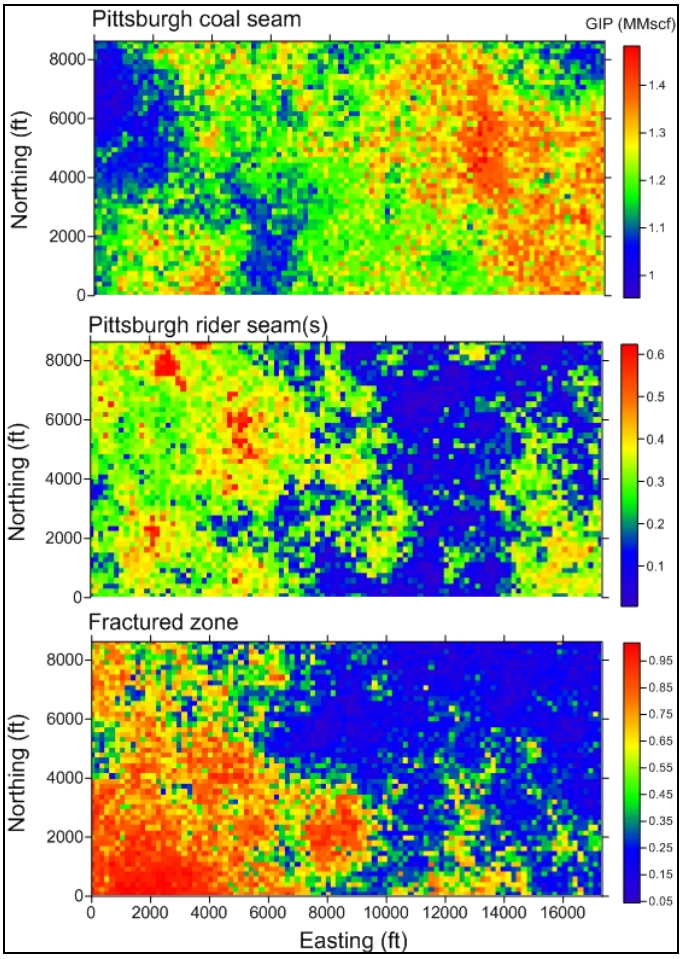

Figure 7. GIP realizations of PCMB, PCR, and fractured zone at Q50.

The fractured zone, on the other hand, is gassier on the left side and towards the bottom of the model area, indicating that these areas should be better controlled using gob gas ventholes. Due to higher gas content, boreholes drilled in high-gas zones can produce methane at higher production rates and can be long-term producers. The minimum, maximum, and mean GIP amounts in the fractured zone are 0.259, 1.689, and 0.919, respectively.

Figure 8 shows the probabilities of GIP occurring more than the estimated mean values of Q50. These probabilities are calculated using all realizations and building a probability density function of estimated values in each grid. Figure 8 clearly shows that certain regions of the model have a very high probability of having more GIP than calculated as the mean for Q50. This indicates that these regions should be the subjects of more focus in designing ventilation and methane removal systems for the PCMB, PCR, and fractured zone.

The uncertainties of total GIP for this model area of the PCMB, PCR, and fractured zone at Q5, Q50, and Q95 are given in Table 5; this shows that the GIP in the PCMB varies from 6174.2 MMscf to 6015.3 MMscf in the model area from Q95 to Q5. This translates to a range value of 158.8 MMscf in the total mining area, or 44.9 Mscf per acre of mining. Caving of the Pittsburgh rider seam, on the other hand, can result in methane emissions in the caved zone from 1,367.6 MMscf to 1,118.2 MMscf (248.8 MMscf) in the Q95 to Q5 interval. Similarly, fractured zone GIP can vary from 4,797.9 to 4,409.4 MMscf (388.5 MMscf) in the Q95 to Q5 quantile interval.

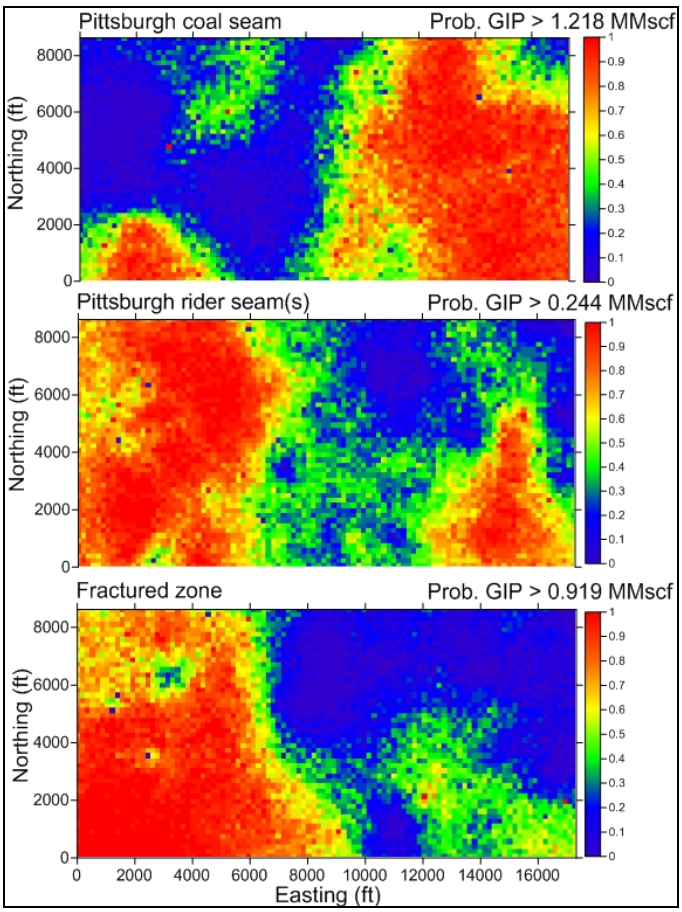

Figure 8. Probabilities of GIPs occurring more than mean values of Q50 in the model area.

Table 5 also shows the amounts of gas-in-place for mining per acre of the Pittsburgh seam in the model area. Overall, mines operating in the Pittsburgh seam in this 3,535-acre area will have a total GIP between 11.5 Bcf and 12.3 Bcf with 5%–95% probability, as shown in Table 5. These GIP quantities amount to 3.26 MMscf and 3.49 MMscf per acre on average for 5% and 95% quantiles, respectively. Therefore, a degasification system using gob gas ventholes and the mine's ventilation system should be designed to collectively handle these amounts of methane, which will originate from mining one acre of PCMB.

Table 5. Total gas-in-place calculated for different quantiles in various zones. The amount of gas-in-place per acre of mining in each of the zones is shown in the bottom half of the table.

Gas-in-place (GIP) MMscf – Model area	Pittsburgh (PCMB)	Rider Seam (PCR)	Fractured Zone (SWC+UNC+WBC)	Total (Bcf)
Q5	6015.4	1118.2	4409.4	11.54
Q50	6091.9	1280.5	4596.1	11.97
095	6174.2	1367.5	4797.9	12.34
GIP per acre of mining (MMscf)				**Total per acre (MMscf)**
Q5	1.702	0.316	1.247	3.26
Q50	1.723	0.362	1.300	3.38
Q95	1.746	0.387	1.357	3.49

An illustration for daily operation of a longwall panel

For this illustration, the GIP of the PCMB and PCR were combined and referred as "mined coal and caved zone" with the premise that the majority of the emissions resulting from these two seams will enter the ventilation system. The GIP map of the fractured zone was taken from the previous section of this paper. Methane from this zone is primarily the source of production for gob gas ventholes.

For both caved and fractured zone GIPs, Q50 values were used as median values. These maps are shown in Figure 9.

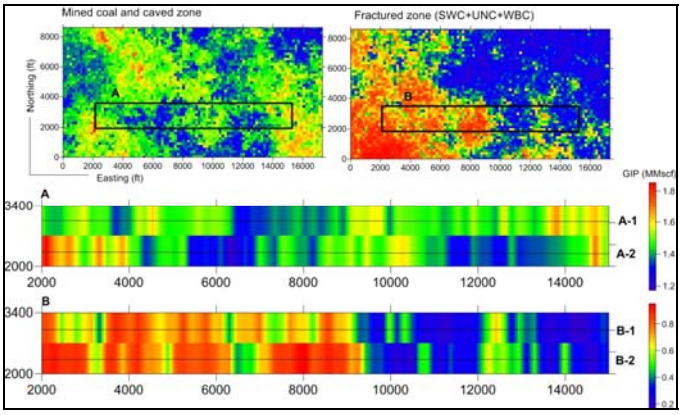

Figure 9. Panel areas outlined in Q50 GIP maps for the mined coal and caved zone and for the fractured zone. The bottom figures (A and B) are the reconstructed panel GIPs based on a daily advance rate of 50 ft.

Two panel areas, both 1,400 ft wide and 13,000 ft long, were outlined, as A and B, in both of the GIP maps to estimate daily average methane emissions (Figure 9). These panel areas were extracted from the maps and re-gridded with 50-ft grids, representing an advance rate of 50 ft per day in the Easting direction using nearest neighbor interpolation. This process created 261 grids, or 261 days, in the East-West direction to complete the panel. Because the panels in this model area were wide, the width of the panels was divided into two to represent each half trip of the shearer during a given day. This process resulted in the reconstructed GIP maps of the caved zone and the fractured zone outlined by the boundaries of the panel. These maps are shown in Figure 9 as A and B.

The advantage of the presented approach in this section, besides quantifying GIP and its uncertainty either on a large area or on a per-acre basis, is that it can be used to predict GIP from the caved zone and from the fractured zone and thus the potential emissions each day during mining of the panel (Figure 9). This may allow ventilation decisions to be made before encountering methane problems.

Figure 10 shows the gas-in-place values traced along the two profiles (each corresponding to an individual day or distance along the panel) on the mined-coal zone and caved zone (A-1 and A-2) panel outline and on the fractured-zone panel outline (B-1 and B-2). These values are the available GIP values from these zones for mining of each of the 50-ft x 700-ft segments. Ventilation and gob gas venthole capacity should be designed accordingly for this panel. These figures show that there are intervals with a GIP as low as 1.2 and as high as 1.7 MMscf per day of mining from the mined and caved zones. There is an interval (10,000–15,000 ft) with relatively low GIP (0.2 MMscf) in the fractured zone. At 9,000 ft, the fractured zone GIP is around 0.7 MMscf, which requires gob drainage.

SUMMARY AND CONCLUSIONS

Successful control of methane gas in the underground coal mine environment requires knowledge of the gas emissions zone, including its size and the gas-in-place quantity. This study used data from 64 exploration boreholes in a mining district in the Northern Appalachian Basin to identify coal layers deemed important for gas emissions into active and inactive longwall mining panels. In the study district, these coal seams included the Pittsburgh Main and Rider coals, the Sewickley coal, the Uniontown coal, and the Waynesburg coal.

This study conducted semivariogram analyses of different attributes using normal score data for exploring spatial correlation of thicknesses and depth. Sequential Gaussian simulations were then performed to obtain spatial distributions of the variables of gas-in-place, which led to their estimations for the various coal layers and important emissions zones of longwall mines at 5%, 50%, and 95% quantiles. For the entire 3,535-acre study area, the 50% values for GIP were 6.1 Bcf, 1.3 Bcf, and 4.6 Bcf in the PCMB, the caved zone, and the fractured zone, respectively. The mine ventilation system and any additional degasification system (if used) should be designed to handle these gas quantities. These quantities represent 1.7 MMscf, 0.4 MMscf, and 1.3 MMscf per acre of mining. Alternatively, by assuming an advance rate of 50 ft per day in a 1,400-ft-long panel, the emissions from these zones can be 2.7 MMscf/day, 0.6 MMscf/day and 2.1 MMscf/day, respectively, per day of mining.

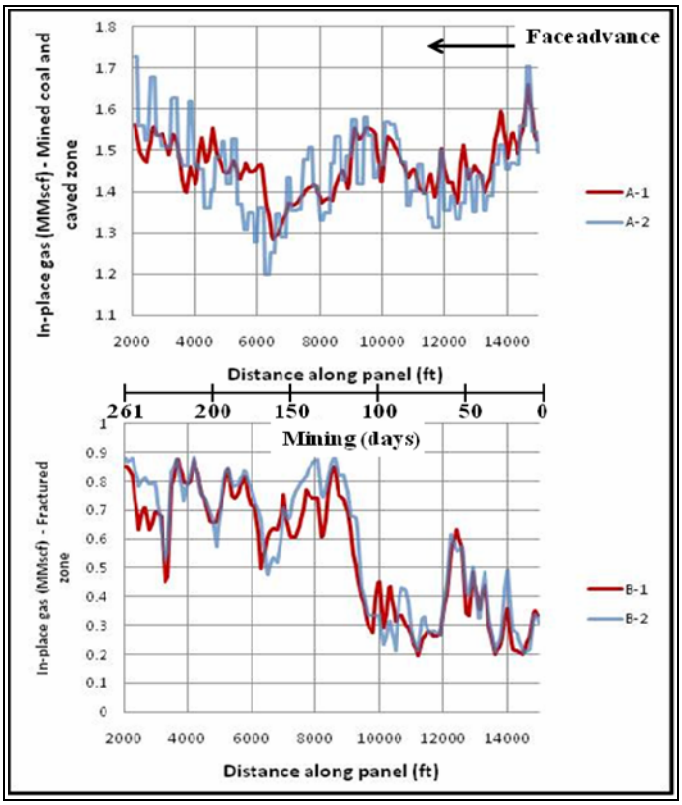

Figure 10. GIP values traced along the A-1/A-2 and B-1/B-2 profiles shown in Figure 9 as daily estimates of methane inflow potential from the caved zone and fractured zone during mining of the panel outlined in Figure 9.

In addition, this study assessed the potential for GIP to impact the day-to-day mine operations by restructuring the GIP map's grids to account for daily advance rates. Such an in-advance estimation of gas-in-place values at different locations of the panel, and thus at different days of operation, can help ventilation engineers and planners to be ready to take necessary precautions before methane increases become a safety threat.

In conclusion, geostatistical modeling and simulation methods are useful in quantitatively evaluating gas-in-place amounts within emissions zones of longwall mines. Geostatistical methods and their estimates can improve ventilation design and increase workers' safety by considering the spatial distributions of gas emissions and their uncertainty. Sequential Gaussian simulation is suited for these applications because the resulting data can be evaluated probabilistically to assess uncertainty.

Disclaimer: The findings and conclusions in this paper are those of the author and do not necessarily represent the views of the National Institute for Occupational Safety and Health. Any commercial product or software mentioned in this paper is not endorsed by NIOSH.

REFERENCES

1. Deutsch CV, Journel AG (1998), "GSLIB Geostatistical Software Library and User's Guide", Oxford University Press. 2nd Edition. New York, NY. 369 pp.

2. Karacan CÖ (2009), “Reservoir rock properties of coal measure strata of Lower Monongahela Group, Greene County (Southwestern Pennsylvania), from methane control and production perspectives”, International Journal of Coal Geology 78, 47-64.

3. Karacan CÖ and Diamond WP (2006), “Forecasting gas emissions for coal mine safety applications”, In: Kissell, F. (Ed.), Handbook for Methane Control in Mining. NIOSH, Information Circular No: 9486, Pittsburgh, PA.

4. Karacan CÖ and Goodman GVR (2011), “Probabilistic modeling using bivariate normal distributions for identification of flow and displacement intervals in longwall overburden”, International Journal of Rock Mechanics and Mining Sciences 48, 27-41.

5. Krishnamoorthy K (2006), “Handbook of Statistical Distributions with Applications”, Chapman and Hall/CRC Press. Boca Raton, Florida. 346 pp.

6. Leuangthong O, Khan KD and Deutsch CV (2008), “Solved Problems in Geostatistics”, Wiley. Hoboken, New Jersey, 207 pp.

7. Markowski A (1998), “Coalbed methane resource potential and current prospect in Pennsylvania”, International Journal of Coal Geology 38, 137-159.

8. Mazza RL and Mlinar MP (1977), “Reducing methane in coal mine gob areas with vertical boreholes”, U.S. Department of the Interior, U.S. Bureau of Mines Research Report No. 1607-1-77.

9. Noack K (1998), “Control of gas emissions in underground coal mines”, International Journal of Coal Geology 35, 57-82.

10. Olea RA (2006), “A six-step practical approach to semivariogram modeling”, Stochastic Environmental Research and Risk Assessment 20, 307-318.

11. Olea RA (2009), “A Practical Primer on Geostatistics”, U.S. Department of the Interior. U.S. Geological Survey, Open-File Report 2009-1103. 346 pp.

12. Remy N, Boucher A and Wu J. (2009), “Applied Geostatistics with SGeMS, A User’s Guide”, Cambridge University Press. Cambridge, United Kingdom. 264 pp.

13. Thakur PC (2006), “Coal seam degasification”, In: Kissell, F. (Ed.), Handbook for Methane Control in Mining. NIOSH, Information Circular No: 9486, Pittsburgh, PA.

14. Webster R and Oliver MA (2007), “Geostatistics for Environmental Scientists”, Wiley. West Sussex, England. 315 pp.